A superhigh discharge capacity induced by a synergetic effect between high-surface-area carbons and a carbon paper current collector in a lithium–oxygen battery*

Luo Guang-Sheng(罗广生)[a)b)], Huang Shi-Ting(黄诗婷)[a)b)], Zhao Ning(赵 宁)[a)b)], Cui Zhong-Hui(崔忠慧)[a)], and Guo Xiang-Xin(郭向欣)[a)†]

[a)] *State Key Laboratory of High Performance Ceramics and Superfine Microstructure, Shanghai Institute of Ceramics, Chinese Academy of Sciences, Shanghai* 200050, *China*

[b)] *University of Chinese Academy of Sciences, Beijing* 100049, *China*

(Received 27 January 2015; revised manuscript received 13 February 2015; published online 20 June 2015)

This paper invesitages the synergetic effect between high-surface-area carbons, such as Ketjan Black (KB) or Super P (SP) carbon materials, and low-surface-area carbon paper (CP) current collectors and it also examines their influence on the discharge performance of nonaqueous Li–O_2 cells. Ultra-large specific discharge capacities are found in the KB/CP cathodes, which are much greater than those observed in the individual KB or CP cathodes. Detailed analysis indicates that such unexpectedly large capacities result from the synergetic effect between the two components. During the initial discharges of KB or SP materials, a large number of superoxide radical ($O_2^{\cdot-}$) species in the electrolytes and Li_2O_2 nuclei at the CP surfaces are formed, which activate the CP current collectors to contribute considerable capacities. These results imply that CP could be a superior material for current collectors in terms of its contribution to the overall discharge capacity. On the other hand, we should be careful to calculate the specific capacities of the oxygen cathodes when using CP as a current collector; i.e., ignoring the contribution from the CP may cause overstated discharge capacities.

Keywords: lithium–oxygen batteries, high discharge capacity, carbon paper current collectors, large-surface carbon-based cathodes, synergetic effect

PACS: 81.05.U–, 81.05.–t, 88.80.ff **DOI:** 10.1088/1674-1056/24/8/088102

1. Introduction

In recent years, the nonaqueous rechargeable lithium-air or lithium–oxygen (Li–O_2) battery has attracted extensive attention because of its ultra-high theoretical energy density (i.e., 3505 $W \cdot h \cdot kg^{-1}$ or 3436 $W \cdot h \cdot l^{-1}$),[1–5] which is about 5–10 times higher than that of state-of-the-art lithium-ion battery.[6–15] Most conventional oxygen electrodes in nonaqueous Li–O_2 batteries are made of coating carbon-based materials with or without catalysts on oxygen-permeable current collectors.[16–21] In previous research, various kinds of carbon materials, such as Ketjan Black (KB),[22,23] or Super P (SP),[24] Vulcan XC-72,[25] carbon nanotubes,[26,27] and graphenes[28,29] have been proven to be good cathode materials for nonaqueous Li–O_2 batteries because they might produce large values of specific capacities during discharge, owing to their intrinsic ability to reduce oxygen, the availability of sufficient active sites for lithium–oxygen reactions, and the spaces for accommodating the insoluble solid products.[30] Carbon papers (CPs), which are composed of densely integrated carbon fibers, have often been used as current collectors since they may be used as light weight conductive supports as well as gas diffusion layers.[31–35] However, few investigations[36] have been carried out on their contribution to discharge capacities.

Consequently, in this work we intentionally choose CPs (TGP-H-060, Toray) as current collectors with different carbon-based cathode materials (e.g. KB or SP). Stainless-steel (SS) mesh current collectors are also used for comparison. It is found that the CP used without cathode materials shows a negligible capacity during discharge. However, a considerable contribution to the discharge capacity by the CP is found when discharging cells with KB or SP-coated CP serving as the cathode. This is attributed to the synergetic effect between the large-surface carbon-based cathode materials and the low-surface CP current collectors. The latter is activated by the initial discharge of the former materials.

2. Experiment

2.1. Electrolyte, electrode preparation, and cell assembly

The electrolyte solvent (tetraethylene glycol dimethyl ether, TEGDME) was dried by freshly activated molecular sieves (4-Å type) for more than one week. The final water content in the TEGDME solvent was below 5 ppm, as mea-

*Project supported by the Natural Science Foundation of the Chinese Academy of Sciences (Grant No. KGZD-EW-202-2), the National Key Basic Research Program of China (Grant No. 2014CB921004), and the National Natural Science Foundation of China (Grant No. U1232111).

†Corresponding author. E-mail: XXGuo@mail.sic.ac.cn

© 2015 Chinese Physical Society and IOP Publishing Ltd

sured by a Metrohm 831 KF Coulometer. The Li salt (lithium bis(trifluoromethylsulfony)imide, LiTFSI, 99.95 %, Aldrich) was baked at 80 °C under vacuum for 48 h. Eventually, the electrolytes were prepared by dissolving 0.9-M LiTFSI in TEGMDE under stirring at room temperature for 24 h, as described in our previous report.[26,27] The high-surface-area KB (KB, EC-600JD), Super P (SP), and low-surface-area CPs (CPs, TGP-H-060) used in the experiment were purchased from AkzoNobel, TIMCAL Graphite & Carbon, and Toray, respectively. The composite oxygen cathodes were made of a slurry consisting of KB or SP carbons and polyvinyl difluoride (PVDF) or polytetrafluoroethylene (PTFE) in a weight ratio of 90:10. The slurry was pasted on CP current collectors with a thickness of approximately 40 μm. After being dried at 80 °C in vacuum for 12 h, the cathodes were punched into small disks with a diameter of 8 mm. The carbon loading was controlled to be 1.0 ± 0.1 mg·cm^{-2}. The average geometric area and mass of the sole CP current collectors were 0.50 cm^2 and 4.35 mg, respectively. Each composite cathode obtained is referred to as KB/CP or SP/CP. In the contrast experiment, the CP current collectors were soaked in a solution of 0.1-M potassium superoxide (KO_2, Aldrich) dissolved in TEGDME for 48 h, and was then washed with ethanol and deionized water. Finally, the prepared CPs were baked at 80 °C under vacuum for 24 h. Swagelok-type cells were assembled in an argon-filled glove box (MBraun, MB-200B) whose moisture and oxygen content was below 0.1 ppm. Each cell consisted of a metallic lithium-foil anode (0.25-mm thick), a glass fiber (Whatman, GF/B) separator, and a carbon-based cathode with a CP or SS current collector. It is worth noting that the cathode was flooded with the liquid electrolyte. Whether the carbon-side (i.e., KB or SP side) of the cathode was configured towards the oxygen atmosphere or towards the lithium anode, no obvious differences in the cell performance were observed.

2.2. Characterizations

After discharge, the air cathodes were taken out from the cells in an argon-filled glove box. They were washed with acetonitrile and protected in a gas-tight device for characterization. Scanning electron microscope (SEM) images and energy-dispersive x-ray spectra (EDX) were collected on an FEI Magellan 400 FESEM with an X-Max Large Area EDX from Oxford Instruments. Fourier transform infrared (FTIR) tests were performed on a Bruker Tensor 27 spectrometer either in transmission mode or in reflection mode by using an anti-reflection unit (ATR) in an argon-filled glove box. The Raman spectra of the KB and treated CP were measured on a Thermo Nicolet DXR spectrometer with a 532-nm excitation wavelength. N_2 adsorption/desorption isotherms were also examined by BET measurement (Macromeritics, ASAP 2010). The x-ray diffraction (XRD) was carried out on a diffractometer (Bruker, D8 Discover) with Cu K_α radiation in a reflection mode. For XRD measurement, the discharged cathodes were sealed in an air-tight sample holder, as described in detail previously.[23,24] Surface compositions of the discharged cathodes were analyzed by using an x-ray photoelectron spectrometer (XPS, ESCAlab-250) with an Al anode source. The galvanostatic discharge and charge behaviors were tested by using a cycler (Arbin BT2000) under the oxygen flowing atmosphere (20 sccm) in a home-made chamber.

3. Results and discussion

The surface morphologies of the two different carbon materials have been investigated. As can be seen in Figs. 1(a)–1(d), the CP consists of carbon fibers, each with a diameter of approximately 10 μm and a smooth surface. However, the KB carbons are composed of spherical primary particles with sizes in a range of 20 nm–50 nm. They are fused together to form high-structure primary agglomerates with sizes that range from 200 nm–300 nm. Their shapes and porosities are dependent on the preparation process. The specific surface area of KB is approximately 10 times larger than that of CP as shown in Fig. 1(e). The Raman spectra of pristine KB and CP are displayed in Fig. 1(f). The G band at 1585 cm^{-1} is observed in both carbon materials. The intensity of the D band at 1350 cm^{-1} of KB is much greater than that of the corresponding G band. However, the D band of CP is nearly invisible. Since the D band is related to the presence of defects, this implies that the KB has more surface defects than the CP. In previous studies,[25,37] the surface defects of carbon cathodes are thought to have had an effect on the discharge performance of a Li–O_2 battery. From the above results, it is reasonable to infer that the two different carbons may have different discharge performances.

Figure 2(a) shows the discharge profiles of the Li–O_2 cells with sole CP, KB/SS, and KB/CP cathodes. It is clear that the sole CP current collector produces a negligible discharge capacity, which is consistent with previous reports.[22,24] In contrast, the cell with the KB/CP shows a much larger discharge capacity of approximately 23 mAh, which is also approximately a factor of 15 greater than that of 1.5 mAh for the cell with the KB/SS. This result clearly indicates that a KB/CP cathode produces a much greater capacity than a cathode of CP or KB alone. More interestingly, a turning point can be clearly seen in the discharge curve of the KB/CP cell. The capacity value (i.e., 1.5 mAh) at the turning point exactly corresponds with that produced by the sole KB in the KB/SS cell. This implies that in the KB/CP cell the initial capacity contribution from the KB layer leads to an additional large capacity, which should be closely related to the CP current collectors.

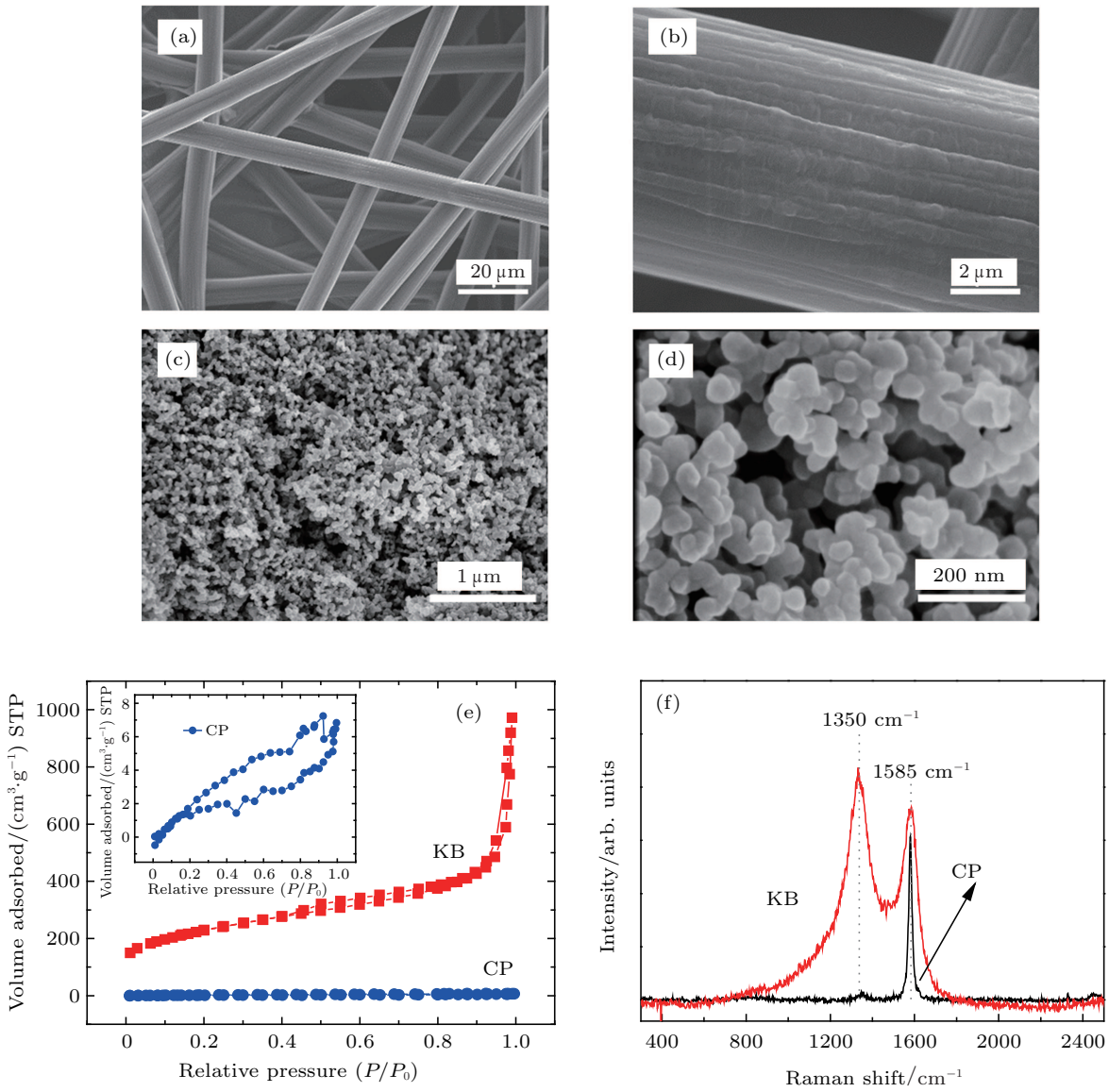


Fig. 1. (color online) SEM images for the pristine ((a) and (b)) CP and ((c) and (d)) KB; (e) N_2 adsorption–desorption isotherm of KB and CP; (f) Raman spectra for KB and CP.

To check whether the above phenomenon is dependent on the current density or the used carbon material, the KB/CP cells are tested at a current density ranging from 50 μA·cm^{-2} to 300 μA·cm^{-2}, the results of which are shown in Fig. 2(b). Different binders (i.e., PVDF and PTFE) and different carbon-based materials (i.e., KB and SP) are also used to construct the air cathodes, the discharge behaviors of which are shown in Figs. 2(c) and 2(d). As can be seen from the above figures, the turning points exist at different current densities, with the corresponding capacity value decreasing with the increasing current density. Similar turning points and an increasing discharge capacity can also be observed if KB:PVDF/CP, KB:PTFE/CP, SP:PVDF/CP, or SP:PTFE/CP are used to construct the cathodes. These results indicate that the underneath CPs are most likely to be activated by the Li_2O_2 or $O_2^{\cdot-}$ intermediate arising from the discharge of the upper-coated cathode materials, such as KB or SP.

To gain an insight into what occurs to the KB/CP cathodes during discharge, compositional and morphological changes are investigated. Figure 3(a) shows SEM images for the cross section of a typical pristine CP. It can be seen that the pristine CP has an apparent thickness of approximate 175 μm, consisting of porous layer-stacked carbon fibers. The coated KB layer on the CP current collector is estimated to be 130 μm in thickness and seems to consist of two parts. One is flatly distributed on the top of CP and the other permeates into the voids, as shown in Fig. 3(b). After the KB/CP cathode discharges to 5 mAh (Fig. 3(c)), the top layer obviously becomes thicker and denser, which is approximately 110 μm. In this process, the total thickness of the cathode increases to ~260 μm. This increase in thickness can be attributed to the expansion of the top layer as a result of the deposited discharge products. After further discharging to 23 mAh (Fig. 3(d)), the

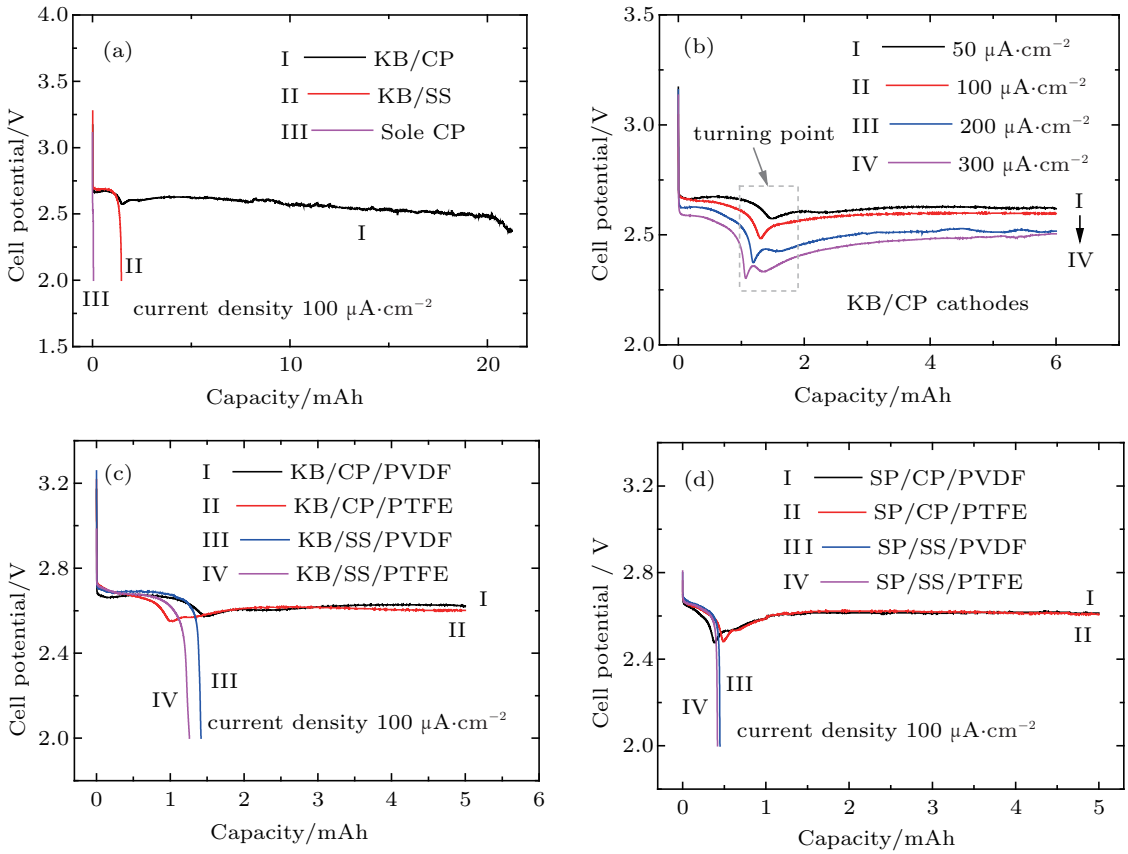


Fig. 2. (color online) Discharge profiles for the Li–O_2 cells: (a) with KB/CP, KB/SS, and CPs as cathodes; (b) with KB/CP as the cathode measured at the current density ranging from 50 μA·cm^{-2} to 300 μA·cm^{-2}; (c) with KB/CP and KB/SS as cathodes; (d) with SP/CP and SP/SS as cathodes. The PVDF ((a) and (b)), PVDF or PTFE ((c) and (d)) are used as the binders, respectively. The current densities in panels (a), (c), and (d) are all 100 μA·cm^{-2}.

cathode is full of discharge product. The CP layer is difficult to distinguish. Meanwhile, the total thickness of the cathode becomes ∼730 μm, which is a factor of 3.5 greater than that of the pristine one as shown in Fig. 3(a). According to Faraday's constant (96485 C·mol^{-1}), we can calculate that the number of transferred electrons for 23 mAh (82.80 C) discharge capacity is 8.58×10^{-4} mol. As the discharge reaction ($2Li + O_2 \rightarrow Li_2O_2$) of Li–$O_2$ cell experiences two electric processes, the discharge product Li_2O_2 is 4.29×10^{-4} mol. With the density (1.21 g·cm^{-3}) and Molar mass (45.88 g·mol^{-1}) of Li_2O_2, the volume of Li_2O_2 can be calculated, which is approximately 1.63×10^{-2} cm^{-3}. On the other hand, we can estimate the volume of the cathode expansion from the cross-section SEM images in Figs. 3(b) and 3(d). We can clearly see that the thickness values for the pristine cathode and after discharging to 23 mAh are 215 μm and 730 μm, respectively, in Figs. 3(b) and 3(d). The average geometric area of the cathode is 0.50 cm^2. Therefore, the expansion of the volume is approximately 2.58×10^{-2} cm^{-3}, which is consistent with the previous calculated value (i.e., 1.63×10^{-2} cm^{-3}). The above results clearly show that the Li_2O_2 formation is initiated first on the large-surface carbons (the top layer, i.e., KB or SP) and then moves on to the low-surface carbon, (i.e., CP). Furthermore, volume expansion of electrode during Li_2O_2 deposition is identified, which should be taken into account for practical design and realization of Li–O_2 cells.

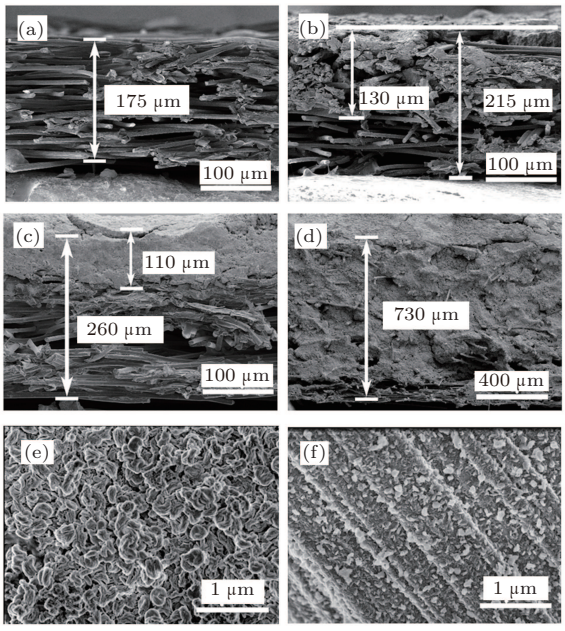


Fig. 3. (color online) Cross-section SEM images of pristine carbon paper (a), pristine cathode of KB/CP (b), cathode after discharging to ∼5 mAh (c), and ∼23 mAh (d); surface morphologies of the KB (e) and CP side (f) at the end of discharge.

The morphologies of discharge products on the KB sur-

face and the surface of CP side are shown in Figs. 3(e) and 3(f), respectively. Toroid-shaped particles can be observed in both cases, meanwhile the former has particles with a greater size than the latter. For the discharge products formed on both sides of the cathodes, composition analyses on both sides are carried out by FTIR, XRD, and XPS respectively. The results are shown in Fig. 4. From the figures, it can be seen that the signal difference between the two sides is negligible. The broadened peaks at 542 cm^{-1} in FTIR (Fig. 4(a)) clearly indicate that Li_2O_2 is the dominant discharge product. The traces of carbonate species (e.g., HCO_2Li and Li_2CO_3) can be identified. Other peaks at 1064, 1138, 1202, and 1340 cm^{-1} are attributed to the used electrolyte (i.e., TEGDME:LiTFSI).[38] The peaks corresponding to the Li_2O_2 crystalline peaks can also be observed by the XRD scans as displayed in Fig. 4(b). The surface-sensitive XPS, on the one hand, confirms that Li_2O_2 is the dominant discharge product (a broad Li–O bond at 55.4 eV as shown in Fig. 4(c)). On the other hand, it indicates that Li_2CO_3 is formed during discharge (a broad Li_2CO_3 peak at approximately 290 eV as shown in Fig. 4(d)). These carbonates formed during discharge are attributed to the decomposition of the used TEGDME electrolyte and/or oxidization of the carbon-based cathode.[39,40]

Therefore, the above analysis clearly indicates that the crystalline Li_2O_2 is formed on both carbon-based cathodes and CP current collectors, although the formed particles seem not to be completely the same in size and morphology. According to the fact that the cathodes of the KB/CP or SP/CP produce much greater capacities than the individuals (as shown in Fig. 2), it is reasonable to assume that these large capacities result from a synergetic effect between the carbon-based cathode materials and the CP current collectors. Furthermore, according to the fact that the discharge capacity contributed from sole CPs is negligible, it should be activated by the effect of the carbon-based cathode, such as KB or SP. It is well known that the KB or SP is a good large-surface material for promoting the reaction of $2Li^+ + O_2 + 2e^- \rightarrow Li_2O_2$, leading to a large amount of Li_2O_2 deposited on the material surfaces as well as O_2^- intermediates dissolved in the solvent. The formed Li_2O_2 at the KB/CP or SP/CP interface may function as pre-deposited nuclei for the CPs, which promotes the further growth of Li_2O_2 on them. As shown in Fig. 5(a), the cell with a pre-deposition of Li_2O_2 on the CP at a small current density (i.e., 5 $\mu A \cdot cm^{-2}$) leads to a much larger discharge capacity (i.e. 0.2 mAh) at 50 $\mu A \cdot cm^{-2}$, which is approximately four times greater than the value (i.e., 0.05 mAh)

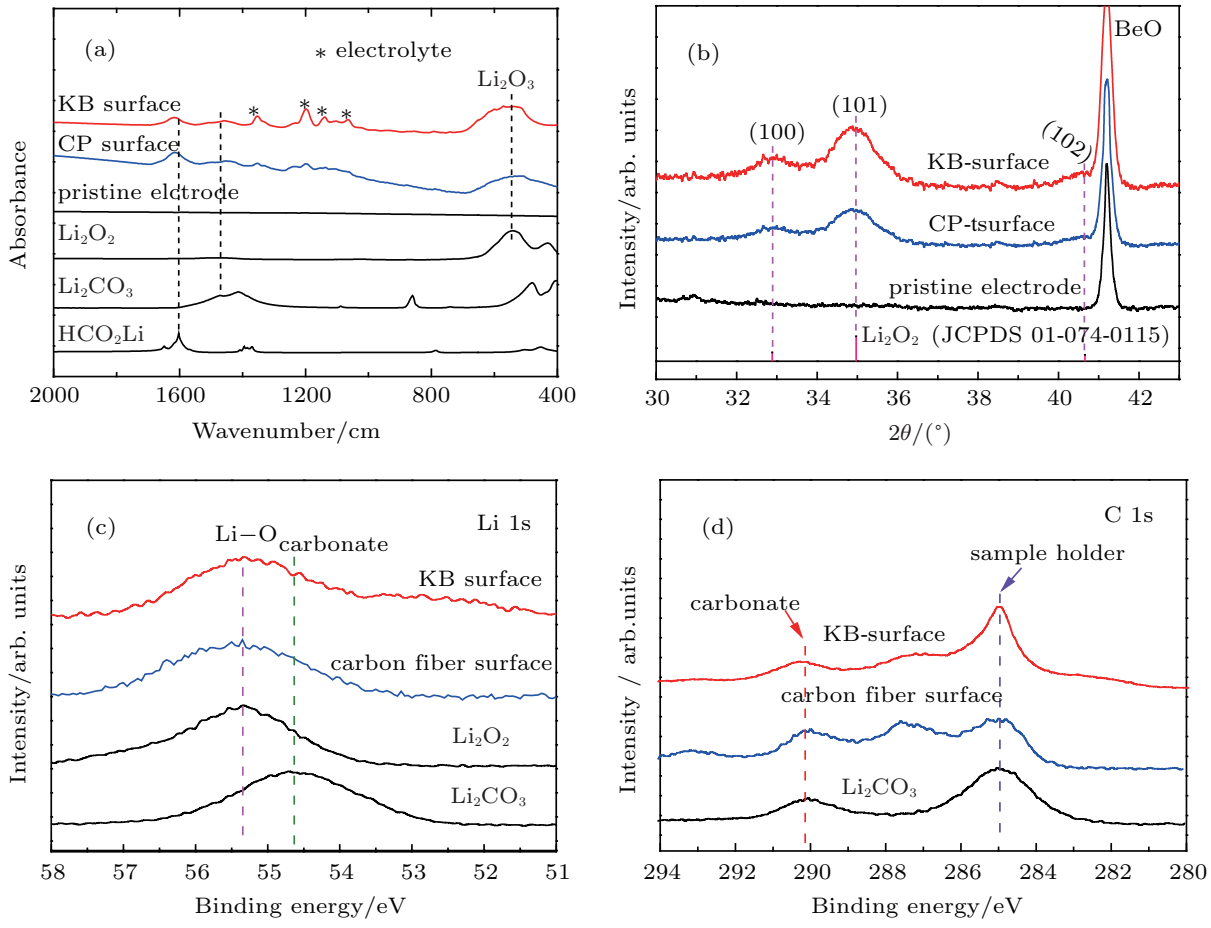


Fig. 4. (color online) (a) FTIR, (b) XRD scans, (c) XPS of Li 1s, and (d) XPS of C 1s spectra for the KB/CP cathodes. The surfaces of KB and CP are both investigated for comparison. The signals of the pristine KB/CP cathodes are also presented for comparison.

without the pre-deposition (as can be seen in Fig. 5(a)). This pre-deposition influence is also observed in the Na–O_2 batteries that were recently reported.[41] Moreover, it is known that the superoxide radicals are produced in the initial discharge process of Li–O_2 cells and dissolved in the liquid electrolyte, which have strong oxidability and may activate the CP surfaces to promote the growth of Li_2O_2 on it. This is indeed observed in the experiment. The KO_2 dissolved in the TEGDME solvent can produce superoxide radicals. In order to simulate the circumstance of electrolyte with superoxide radicals in discharge process, the CPs were soaked in 0.1-M KO_2/TEGDME solvent for 48 h. After being washed and dried, the treated CPs are used as cathodes to assemble the cells. As can be seen in Fig. 5(b), the discharge capacity (0.16 mAh) of the treated CPs is approximately three times larger than that (0.05 mAh) of the pristine CPs, clearly indicating the promotion effect on growth of Li_2O_2 on the CP by the O_2^- in the solvent. Consequently, these two factors cause the CPs to produce considerable discharge capacities.

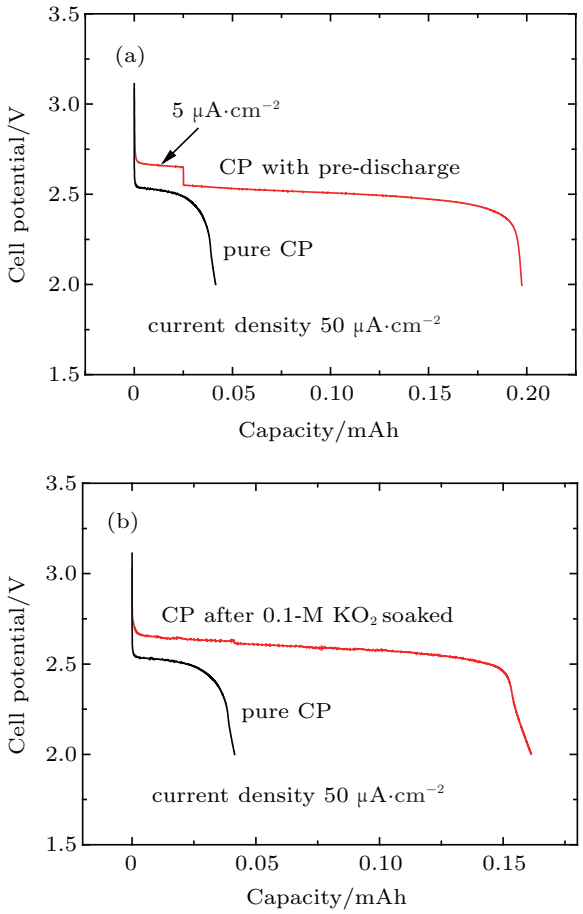


Fig. 5. (color online) Discharge profiles for the Li–O_2 cells (a) with a pre-deposition of thin Li_2O_2 layer at 5 μA·cm^{-2}; (b) treated with 0.1-M KO_2/TEGMDE solvent, at a current density of 50 μA·cm^{-2}.

The turning points as shown in Fig. 2 can be explained by the fact that the Li_2O_2 preferentially grows at the large-surface carbon material (e.g. KB or SP) during the initiate discharge. After the carbon materials all form Li_2O_2 compounds and their active sites are used up, the growth of Li_2O_2 on the low-surface carbon fibers becomes dominant, as shown in Fig. 3. Since the sizes and morphologies of the formed Li_2O_2 particles are not completely the same for carbon-based cathode materials and carbon fibers, different discharge plateaus lead to the turning points, as observed in the discharge curves. As indicated in the discussion on the properties of KB and CPs, these results are probably caused by the fact that the surface morphologies and chemical defects are different in the two types of carbon materials.

The reason why CP current collectors can be activated to contribute a large discharge capacity lies in two key points: the first is that the synergetic effect between the large-surface carbon material and the low-surface carbon–paper current collector could be used to enhance the discharge capacity of the Li–O_2 battery; and, the second is that the discharge capacities of the investigated cathode materials could be overestimated if the mass of CP is excluded. For instance, a discharge capacity of an Li–O_2 cell based on the sole weight of KB would be as large as 2×10^4 mAh·g_{KB}^{-1}. Whereas, the value is only 2500 mAh·g_{KB+CPs}^{-1} if both weights of the KB and CPs are included. This overstated capacity may also be misleading in the case of cycling with limited depth of discharge (DOD). As can be seen in Fig. 6, if the limited discharge capacity of 1000 mAh·g^{-1} is only for the weight of KB, then the cells can be cycled

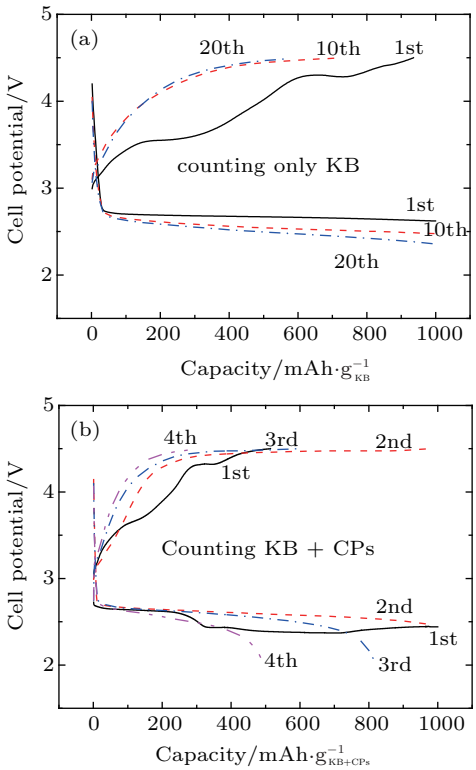


Fig. 6. (color online) Cycle performances of a Li–O_2 battery under different specific capacity limits based on (a) the KB carbon weight (1000 mAh·g_{KB}^{-1}) and (b) the overall cathode weight (1000 mAh·g_{KB+CPs}^{-1}). The current density that we used for all of the measurements is 100 μA·cm^{-2}.

at least 20 times without capacity degradation. However, if 1000 mAh·g^{-1} is for both weights of KB and CPs, then the cells can only be cycled a few times in terms of maintaining initial capacity. This lies in the fact that the former DOD is only 5% while the latter is 50% of the overall discharge capacity. A smaller DOD obviously leads to an extended cycle number. This result means that we should be careful calculating discharge capacities when CPs are used as current collectors.

4. Conclusions

We have investigated the synergetic effect and discharge behaviors of Li–O_2 cells with CPs as current collectors and KB or SP as cathode materials. We have found that the CPs can contribute unexpectedly large discharge capacities. The morphology and chemical analyses of the discharged cathodes reveal that a large number of Li_2O_2 particles are formed on the carbon fibers of CP. The formed Li_2O_2 particles (before the turning point) on the carbon-based cathode material (e.g., KB or SP) and intermediate O_2^- dissolved in the liquid electrolyte activate the CPs below. This synergetic effect between the carbon-based cathode material and the CP current collector is responsible for the observed ultra-large discharge capacity. These results indicate, on the one hand, that the contribution of CP current collector sometimes should not be excluded in order to avoid the overstated discharge capacity of the studied cathode material. On the other hand, CP would be a good material for use as a current collector because it could make a contribution to the overall discharge capacity.

References

[1] Abraham K M and Jiang Z 1996 *J. Electrochem. Soc.* **143** 1

[2] Bruce P G, Freunberger S A, Hardwick L J and Tarascon J M 2012 *Nat. Mater.* **11** 19

[3] Liu Y L, Wang R, Lyu Y C, Li H and Chen L Q 2014 *Energy Environ. Sci.* **7** 677

[4] Dong S M, Wang S, Guan J, Li S M, Lan Z G, Chen C, Shang C Q, Zhang L X, Wang X G, Gu L, Cui G L and Chen L Q 2014 *J. Phys. Chem. Lett.* **5** 615

[5] Zheng H, Xiao D D, Li X, Liu Y L, Wu Y, Wang J P, Jiang K L, Chen C, Lu L, Wei X L, Hu Y S, Chen Q and Li H 2014 *Nano Lett.* **14** 4245

[6] Yu P F, Cui Z H, Fan W G and Guo X X 2013 *Chin. Phys. B* **22** 038101

[7] Whittingham M S 2014 *Chem. Rev.* **114** 11414

[8] Pan H L, Hu Y S, Li H and Chen L Q 2011 *Chin. Phys. B* **20** 118202

[9] Guo X X, Huang S T, Zhao N, Cui Z H, Fan W G, Li C L and Li H 2014 *J. Inorg. Mater.* **29** 113 (in Chinese)

[10] Dong S M, Chen X, Zhang K J, Gu L, Zhang L X, Zhou X H, Li L F, Liu Z H, Han P X, Xu H X, Yao J H, Zhang C J, Zhang X Y, Shang C Q, Cui G L and Chen L Q 2011 *Chem. Commun.* **47** 11291

[11] Zhou X S, Dai Z H, Liu S H, Bao J C and Guo Y G 2014 *Adv. Mater.* **26** 3943

[12] Zhou X S, Bao J C, Dai Z H and Guo Y G 2013 *J. Phys. Chem. C* **117** 25367

[13] Huang L X, Chen Y F, Li P J, Huan R, He J R, Wang Z G, Hao X, Liu J B, Zhang W L and Li Y R 2012 *Acta Phys. Sin.* **61** 156103 (in Chinese)

[14] Chen C, Ru Q, Hu S J, An B N and Song X 2014 *Acta Phys. Sin.* **63** 198201 (in Chinese)

[15] Xu S Y, Wu X Y, Li Y M, Hu Y S and Chen L Q 2014 *Chin. Phys. B* **23** 118202

[16] Christensen J, Albertus P, Sanchez-Carrera R S, Lohmann T, Kozinsky B, Liedtke R, Ahmed J and Kojic A 2012 *J. Electrochem. Soc.* **159** R1

[17] Shao Y Y, Ding F, Xiao J, Zhang J, Xu W, Park S, Zhang J G, Wang Y and Liu J 2013 *Adv. Funct. Mater.* **23** 987

[18] McCloskey B D, Speidel A, Scheffler R, Miller D C, Viswanathan V, Hummelshøj J S, Nørskov J K and Luntz A C 2012 *J. Phys. Chem. Lett.* **3** 997

[19] Peng Z Q, Freunberger S A, Chen Y H and Bruce P G 2012 *Science* **337** 563

[20] Meini S, Piana M, Beyer H, Schwämmlein J and Gasteiger H A 2012 *J. Electrochem. Soc.* **159** A2135

[21] Guo X X and Zhao N 2013 *Adv. Energy Mater.* **3** 1413

[22] Jung H G, Hassoun J, Park J B, Sun Y K and Scrosati B 2012 *Nat. Chem.* **4** 579

[23] Cui Z H and Guo X X 2014 *J. Power Sources* **267** 20

[24] Xu J J, Wang Z L, Xu D, Zhang L L and Zhang X B 2013 *Nat. Commun.* **4** 2438

[25] Yang W, Salim J, Ma C, Ma Z H, Sun C W, Li J Q, Chen L Q and Kim Y 2013 *Electrochem. Commun.* **28** 13

[26] Cui Z H, Fan W G and Guo X X 2013 *J. Power Sources* **235** 251

[27] Fan W G, Cui Z H and Guo X X 2013 *J. Phys. Chem. C* **117** 2623

[28] Xiao J, Mei D H, Li X L, Xu W, Wang D Y, Graff G L, Bennett W D, Nie Z M, Saraf L V, Aksay I A, Liu J and Zhang J G 2011 *Nano Lett.* **11** 5071

[29] Wang L X, Ara M, Wadumesthrige K, Salley S and Ng K Y S 2013 *J. Power Sources* **234** 8

[30] Lu Y C, Xu Z, Gasteiger H, Chen S, Hamad-Schifferli K and Yang S H 2010 *J. Am. Chem. Soc.* **132** 12170

[31] Zhai D, Wang H H, Yang J, Lau K C, Li K, Amine K and Curtiss L A 2013 *J. Am. Chem. Soc.* **135** 15364

[32] Wu D F, Guo Z Y, Yin X B, Pang Q Q, Tu B B, Zhang L J, Wang Y G and Li Q W 2014 *Adv. Mater.* **26** 3258

[33] Luo Z K, Liang C S, Wang F, Xu Y H, Chen J, Liu D, Sun H Y, Yang H and Fan X P 2014 *Adv. Funct. Mater.* **24** 2101

[34] Hassoun J, Jung H G, Lee D J, Park J B, Amine K, Sun Y K and Scrosati B 2012 *Nano Lett.* **12** 5775

[35] Xu L, Ma J, Li B H and Kang F Y 2014 *J. Power Sources* **255** 187

[36] Geaney H, O'Connell J, Holmes J D and O'Dwyer C 2014 *J. Electrochem. Soc.* **161** A1964

[37] Huang S T, Fan W G, Guo X X, Meng F H and Liu X Y 2014 *ACS Appl. Mater. Interfaces* **6** 21567

[38] Gowda S R, Brunet A, Wallraff G M and McCloskey B D 2013 *J. Phys. Chem. Lett.* **4** 276

[39] Freunberger S A, Chen Y, Drewett N E, Hardwick L J, Bardé F and Bruce P G 2011 *Angew. Chem. Int. Ed.* **50** 8609

[40] Thotiyl M M O, Freunberger S A, Peng Z and Bruce P G 2013 *J. Am. Chem. Soc.* **135** 494

[41] Zhao N, Li C L and Guo X X 2014 *Phys. Chem. Chem. Phys.* **16** 15646